Correlation between the plasma characteristics and the surface chemistry of plasma-treated polymers through partial least squares analysis



LABORATOIRE LIS D'INGÉNIERIE DE SURFACE

Maryam Mavadat[1,2], Massoud Ghasemzadeh-Barvarz[3], Stéphane Turgeon[2], Carl Duchesne[3], and Gaétan Laroche[1,2]

[1]Laboratoire d'Ingénierie de Surface, Département de génie des mines, de la métallurgie et des matériaux, Centre de Recherche sur les Matériaux Avancés, 1065, avenue de la Médecine, Université Laval, Québec, Canada G1V 0A6
[2]Centre de recherche du CHU de Québec, Hôpital Saint-François d'Assise, 10, rue de l'Espinay, Québec, Canada G1L 3L5
[3]Département de génie chimique, 1065, avenue de la Médecine, Université Laval, Québec, Canada G1V 0A6

ABSTRACT

We investigated the effect of various plasma parameters (relative density of atomic N and H, plasma temperature and vibrational temperature) and process conditions (pressure and $H_2/(N_2+H_2)$ ratio) on the chemical composition of modified poly(tetrafluoroethylene) (PTFE). The plasma parameters were measured by means of near-infrared (NIR) and UV-visible emission spectroscopy with and without actinometry. The process conditions of the N_2-H_2 microwave discharges were set at various pressures ranging from 100 to 2000 mTorr, and $H_2/(N_2+H_2)$ gas mixture ratios between 0 and 0.4. The surface chemical composition of the modified polymers was determined by X-ray photoelectron spectroscopy (XPS). A mathematical model was constructed using the partial least squares regression algorithm to correlate the plasma information (process condition and plasma parameters as determined by emission spectroscopy) with the modified surface characteristics. To construct the model, a set of data input variables containing process conditions and plasma parameters were generated, as well as a response matrix containing the surface composition of the polymer. This model was used to predict the composition of PTFE surfaces subjected to N_2-H_2 plasma treatment. Contrary to what is generally accepted in the literature, the present data demonstrate that hydrogen is not directly involved in the defluorination of the surface but rather produces atomic nitrogen and/or NH radicals which are shown to be at the origin of fluorine atom removal from the polymer surface. The results show that process conditions alone do not suffice in predicting the surface chemical composition and that the plasma characteristics, which cannot be easily correlated with these conditions, should be considered. Process optimization and control would benefit from plasma diagnostics, particularly infrared emission spectroscopy.

CITATION

Mavadat, M., Ghasemzadeh-Barvarz, M., Turgeon, S., Duchesne, C., & Laroche, G. (2013). Correlation between the plasma characteristics and the surface chemistry of plasma-treated polymers through partial least-squares analysis. Langmuir, 29(51), 15859-15867.

This is the author's version of the original manuscript. The final publication is available at ACS Langmuir Link Online via doi.org/10.1021/la403822a

1 INTRODUCTION

The use of polymers in biomedical applications requires that their volume and surface properties be fine-tuned independently. In this context, plasma technology has become the tool of choice to specifically modify the outermost surface layer of polymers without altering their bulk.

More specifically, plasma surface modification is used to improve the surface properties of poly(tetrafluoroethylene) (PTFE) through the introduction of amino groups that are thereafter used to conjugate biocompatible molecules. Accordingly, various kinds of plasmas with different atmospheres, such as N_2-H_2 and NH_3, are used for polymer surface modification. On one hand, due to the multitude of basic reactions occurring simultaneously, it is impossible in most cases to calculate in detail the physical and chemical behavior of plasma in interaction with the surface. On the other hand, different plasma parameters, such as pressure, power, and gas mixture, affect the results of the modified surface[1]. Consequently, it is difficult to predetermine the variety of functional groups formed in a plasma treatment to a well-defined set of species.

Optimizing surface treatments therefore requires a comprehensive follow-up of each reaction parameter so as to maximize the concentration of the desired species while minimizing surface damage. This optimization calls for an extensive characterization of the modified surfaces and of the plasma-polymer interaction through various surface characterization methods, such as X-ray photoelectron spectroscopy (XPS) which requires a huge amount of time. In the case of amino functional groups, specifically, chemical derivatization procedures are mandatory. Moreover, upscaling a plasma process from laboratory to industrial dimensions is far from being a straightforward procedure.

Plasma diagnostic methods combined with surface characterization are therefore warranted to better under-stand plasma-surface modification processes, with plasma parameters serving fundamental studies to optimize experimental process conditions. In this context, determining the key plasma parameters which have a significant effect on the surface is a prerequisite for further process control. Indeed, the concentration and energy of species in the plasma have been shown to drive the nature and concentration of the resulting surface-grafted moieties. In this regard, Wang et al. found a direct correlation between the observed NH emission peak intensity at 336.0 nm in a N_2-H_2 discharge and the amino group density found on the surface[2], while Favia et al. found a direct relationship between the N/C and NH_2/N surface ratio, with the relative density of N-containing species (N_2, NH), and H atoms detected in a glow discharge using actinometry[3]. These results were based on UV-visible emission spectroscopy data and subsequent conclusions through a quantitative comparison of the plasma emission data and the resulting surface chemistry.

The goal of this study was to correlate the process conditions and plasma parameters with the PTFE surface chemistry by applying a multivariate analysis to broaden the understanding of the surface plasma treatment process. This correlation may ultimately be used to predict N, F, C and NH_2 surface concentrations from in-formation originating from the plasma.

Plasma parameters which may have a significant effect on the resulting surface were thus determined. Various plasma parameters can in fact be monitored through plasma characterization. According to the literature and considering the final goal of this research, some of these parameters are directly measurable by both UV-visible and near infrared emission spectroscopy, which provide complementary information. Thus far, very few studies have used infrared emission spectroscopy to characterize gaseous plasmas[4,5].

Nitrogen and hydrogen atomic concentration in the discharge may have a significant effect on the surface chemistry of plasma-modified materials[6]. Various species energy levels (referred to as temperatures) may also influence the resulting plasma-treated surface chemistry. On one hand, the discharge chemistry is influenced by gas temperature, as it governs the reaction rate of active species generation through dissociation, excitation and ionization processes. On the other hand, vibrational temperature of the species in the plasma may also be of prime importance because it governs the kinetics of the excited particles.

In addition to these data, which can be measured experimentally, the plasma environment can also be de-scribed through process conditions such as gaseous pressures and N_2-H_2 ratios in the gas. In this study, total pressure was changed between 100 and 2000 mTorr for different relative concentrations of hydrogen (0% to 40%) which were adjusted through partial pressure measurements. Thereafter, these so-called plasma characteristics were correlated with the surface chemistry in terms of N, F, C, and NH_2 concentration, as determined by XPS, using the projection to latent structures regression, also known as the partial least squares regression, (PLSR). This was achieved by correlating an input matrix built with an input variable data set containing the plasma characteristics measured from several experiments with a response matrix containing the surface con-centration results of the various films.

2 THEORETICAL ASPECTS

2.1 Plasma optical emission spectroscopy

Optical emission spectroscopy (OES), which is an in situ nonintrusive diagnostic method, is probably the most widely used method for monitoring and diagnosing plasma processes[7]. By measuring the wavelengths and intensities of emitted spectral lines, the nature of the particles and ions present in the plasma can be deduced. Because light emission is an inherent characteristic of plasma, the setup to detect the information is simpler than that of other methods. Moreover, light emission from the species in the plasma contains plenty of useful information on the chemical and physical processes occurring in the plasma and therefore plasma characterization.

2.1.1 Plasma optical emission actinometry

Plasma optical emission actinometry is a technique of choice to estimate the relative concentration of the atomic species (in this case, hydrogen and nitrogen) in the plasma. This semi-quantitative technique has been applied and explained in great detail in numerous studies[7,8] . Briefly, when the plasma process conditions (power, pressure, or gas composition) are altered, the intensity of the emitted line arising from atomic transitions cannot be assumed to be proportional to the density of the ground state species, because the intensity of the emitted lines (or the excitation efficiency) depends not only on the density of the ground state species but also on the excitation cross section and electron energy distribution function (EEDF). Actinometry is a relatively simple procedure designed to rid the effect of plasma excitation efficiency from the OES data. In this technique, a small quantity (1–3%) of a gas, most likely a rare gas (called actinometer) is mixed in with the gas fed to the plasma. The actinometer gas concentration is known and maintained constant and the optical emission arising from it is used as an internal standard to measure the excitation efficiency of the plasma when the process parameters are altered. Having said that, performing actinometry requires that the excitation takes place through electron collisions, a similar excitation threshold between the atomic species of interest and the actinometer, and a light-emitting deexcitation process.

In this study, we used the near infrared part of the emission spectrum to determine the relative density of atomic nitrogen and hydrogen in the discharge as a function of plasma process conditions.

2.1.2 Plasma temperature

As explained in the previous section, plasma temperature is another key plasma parameter affecting the chemistry of the discharge and consequently, the chemistry of the modified surface. As N_2 molecules exchange rotational and translational energy faster with heavy particles than with electrons, it is possible that rotational distributions quickly achieve thermodynamic equilibrium with the bulk gas. A convenient way to determine T_g for these plasmas is by measuring the rovibrational

spectrum of nitrogen. Even for plasmas containing no nitrogen, the rovibrational band spectrum of nitrogen can be used as a sensitive "thermometer" for gas temperature by adding trace amounts of N_2, i.e., a molecular actinometer.

Due to its simplicity and high sensitivity, optical emission spectroscopy is the most common means to determine rotational temperature of different types of discharges and a wide range of working conditions. In theory, the rotational temperature of N_2 can be determined using various bands from either the first negative[9], second positive (2nd positive)[10], or first positive (1st positive) systems[8] through a Boltzmann plot, provided that the spectrometer resolution is high enough to separate the rotational structure of the bands or by fitting numerical models to the band envelope when medium to low resolution spectrometers are used[4,8].

The method we used to determine gas temperature was based on the near-IR region of the spectrum and has been previously presented elsewhere[8]. Briefly, the plasma gas temperature was evaluated by calculating and generating a theoretical spectrum closely matching the bands originating from the 0-0 transition in the N_2 1st positive system, which was observed in the range of 1025-1055 nm. To this end, a synthetic spectrum generated in MATLAB™ was used. This procedure, however, required a knowledge of FTIR spectrometer apparatus operations, which in turn had to be convolved with the calculated spectrum. The shape parameters of the 826 nm Ar line taken from the spectrum of an Ar-Hg source were therefore used, which enabled us to determine the instrumental broadening for the experimental setup used in the present study[11].

2.1.3 Characteristic vibrational temperature $\theta_1(X)$ of $N_2(X, v)$ from the vibrational distribution of $N_2(C, v')$.

Because the kinetics of the particles are related to their vibrational temperature, this plasma parameter could somewhat influence the chemistry of the plasma treated surface. The vibrational temperature of molecules can be determined from the vibrational band intensities. In plasma containing nitrogen, a vibrational temperature of $N_2(C)$ can be determined by considering its Boltzmann distribution. Moreover, in the case of direct electron excitation of $N_2(C)$ from the ground state $N_2(X)$, the ground state vibrational temperature $T_v(X)$ can also be determined. To do this, the Franck-Condon (FC) factors are used to establish the relationship between the $N_2(C, v')$ and $N_2(X, v)$ vibrational states. The vibrational temperature of $N_2(X)$ represents the vibrational energy of the ground state species in the plasma. Because the density of the ground state species in the plasma is vastly more important than that of the excited species, the non-excited species could have more influence on the plasma modified surface. The vibrational aspects of plasmas are well documented in the literature[12].

In the present study, T_{vib} was determined from the 2nd positive system of $N_2(C, v')$ by considering the sequence of $\Delta v = -2$ vibrational transition in the UV-visible spectral region. Taking into account the direct excitation of $[C, v']$ from $[X, v']$ by electron collisions, and assuming a Treanor distribution for the $N_2(X, v)$ vibrational levels, the distribution $f(v)$ was calculated from the following analytical equation[12]:

$$f(v) = f(0) \exp -v \left(\frac{E_{10}}{\theta_1^X} - (v-1) E_{10} \frac{\delta}{T_g} \right) \quad (1)$$

with

$$f(0) = 1 - exp\left(\frac{-E_{10}}{\theta_1^X} \right)$$

where θ_1^X is the characteristic vibrational temperature of the two states, $N_2(X, v = 0 - 1)$, δ is the coefficient of anharmonicity, and $E_{10} = E(X, 1) - E(X, 0)$. For $N_2(X)$, $E_{10} = 3396K$ and $\delta = 6.22 * 10^{-3}$ [13].

Continuing with the same consideration, according to the Frank-Condon (FC) principle (instantaneous collisions), the electron excitation rates were therefore replaced by FC factors. The stationary relative $[C, v']$ population is thus described as:

$$[C, v'] = \sum_v \frac{[X,v]q(X,v-C,v')}{v(C,v')} \quad (2)$$

With $q(X, v - C, v')$ as the FC factor , $v\,(C, v') = v_R(C, v') + N_0 k_Q(C, v')$, where $v_R(C, v')$ is the radiative frequency in reference [14] and $k_Q(C, v')$ is the quenching rate of the $[C, v']$ states, with N_2 in reference[15]. Equation (2) makes it possible to calculate the normalized vibrational distribution, $[C, v']/[C, 0]$ for $\theta_1^X = 1000 - 30000K$. On the other hand, $[C, v']/[C, 0]$ can be measured experimentally for each plasma process condition to compare with the calculated results in order to deduce θ_1^X.

2.2 Multivariate statistical analyses

Traditionally, multiple linear regression (MLR) is used to model a response matrix (Y**)** by means of a predictive (X) matrix, as long as only a few X-variables are available and are fairly uncorrelated [16]. However, as plasma process conditions and emission spectroscopy results (the X-variables) are correlated, partial least square regression (PLSR) approaches should definitely be privileged. In fact, the prediction by PLSR is achieved by extracting, from X, a set of orthogonal components defined as linear combinations of the original X-variables. These so-called latent variables (or main components) relate the two blocks of variables, namely, X and Y in a way that maximizes the covariance between them[17]. In other words, these linear combinations are the most predictive of Y.

The objective of PLSR is actually to model the relationships between the X (N × K) and Y (N × M) matrices as well as within each data block, through the following bilinear decomposition[18]:

$$X = TP' + E \quad (3)$$

$$Y = TQ' + F \quad (4)$$

$$T = XW^* \quad (5)$$

where P (K × r) and Q (M × r) are the loading matrices for the X and Y spaces, respectively, and W* is the so-called weight matrix containing those linear combinations of X-variables that are the most predictive of Y. The results of calculating the linear combinations of the X-variables for each observation (i.e., row of X) are stored in the score matrix T. The model residuals for the X and Y data are collected in the E and F matrices, respectively.

For prediction purposes, Equations 3-5 can be rewritten in a form similar to that of a multiple regression model:

$$Y = XW^*Q' + F = XB + F \quad (6)$$

The PLS-regression coefficients, B, are represented as follows:

$$B = W^{*} Q' \tag{7}$$

PLSR modeling also makes it possible to quantify the importance of each variable in the projection model, thus enabling the identification of the relative importance of the input variables in a given process, such as a plasma surface modification. This is achieved by calculating the variable importance on the projection (VIP)[19]:

$$VIP_k = \sqrt{\frac{K \sum_{a=1}^{r} \left(\left(\frac{w_{ak}}{\|w_a\|} \right)^2 (q_a^2 t_a' t_a) \right)}{\sum_{a=1}^{r} \left(q_a^2 t_a' t_a \right)}} \tag{8}$$

where K is the total number of variables, w_{ak} is the weight of the k^{th} variable for principal component a, r is the number of the principal component, and w_a, t_a and q_a are the a^{th} column vectors of W, T and Q, respectively.

According to Eriksson et al., the variables with a VIP greater than 1 have more influence in the model because the average of the squared VIPs is equal to 1[18]. The variables with a VIP between 0.8 and 1.0 have moderate influence variables, while a VIP less than 0.8 are less important variables. For more details on PLSR, the reader is referred to Wold et al.[16].

3 MATERIALS AND METHODS

3.1 Materials and processes

3.1.1 Materials

The microwave reactor for the experiments was purchased from Plasmionique Inc. (Varennes, QC, Canada). The feed gases used for the plasma treatments were N_2 gas (99.998% purity), H_2 gas (99.999% purity) and Ar gas (99.999% purity), all purchased from Linde Canada (Quebec, QC, Canada).

Commercial flat sheets of poly(tetrafluoroethylene) (PTFE) 250 µm in thickness were purchased from Good-fellow Corp. (Devon, PA, USA) and cut into squares with 20 mm sides. Prior to surface modification, the polymer samples were successively cleaned ultrasonically for 10 min in acetone, deionized water, and methanol. The films were then air-dried and kept under vacuum prior to use. The amine surface concentration was ascertained through derivatization using 98% chlorobenzaldehyde obtained from Sigma Aldrich Canada Ltd. (Oakville, ON, Canada).

3.1.2 Plasma treatment

The tests were performed on a downstream discharge for the surface modification of the samples by means of low-pressure microwave plasma. The substrate was located near the plasma zone in the vacuum chamber. The process gases entered the vacuum chamber through a quartz tube (internal diameter = 32 mm) crossing a rectangular waveguide resonant cavity to which the microwave radiation (frequency: 2.45 GHz) was applied.

The pressure range was pre-determined at between 100 and 2000 mTorr. For a pressure lower than 100 mTorr, igniting the plasma was too difficult, compared to the surface treatment for a pressure higher than 2000 mTorr which was not significant. In addition, as most modifications

occurred when the H_2 concentration was less than 20%, and because the possibility of plasma etching was more significant than modification for a H_2 concentration higher than 40%, the H_2 minimum and maximum limits were chosen at 0% and 40%, respectively.

The treatment time during the entire experiments was set at 3 minutes. In fact, preliminary experiments determined the best treatment time in order to optimize surface modification while minimizing the substrate damage.

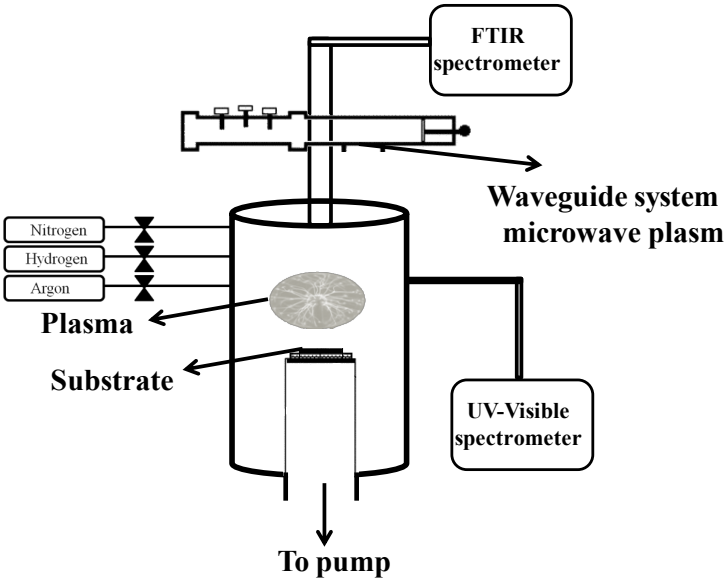


Figure 1. Experimental setup.

3.1.3 Surface characterization

Surface chemical composition was investigated by means of X-ray photoelectron spectroscopy (XPS) using a PHI 5600-ci spectrometer (Physical Electronics USA, Chanhassen, MN). The PTFE films were analyzed both before and after plasma treatment, as were all of the surfaces that underwent chemical derivatization. A standard (non-monochromatized) aluminum X-ray source (Al Kα=1486.6 eV) was used at 200 W to record the survey spectra (1200–0 eV). The detection angle was set at 45^o with respect to the normal of the surface, and the analyzed area was 0.005 cm^2. Five spectra were obtained for the samples before and after surface modification. Each experiment was performed in triplicate for each process condition.

As XPS analyses did not directly reveal the nature of the N-species grafted onto the surface (the chemical shifts were not significantly different), chemical derivatization was thus performed. The derivatization technique makes it possible to calculate the amount of amine grafted onto a surface. Briefly speaking, a selective chemical reaction is induced between surface moieties created through plasma treatment (amino groups, in this case) and a chemical reagent (4-chlorobenzaldehyde, in this case) bearing at least one atom which is not present on the treated surface (chlorine, in this case). Following surface derivatization, the XPS signal from chlorine atom can be used to quantify the surface concentration of the derivatized surface moieties.

Three spectra were obtained for each sample following chemical derivatization. Each experiment was per-formed in triplicate for each process condition.

3.1.4 Plasma emission spectroscopy

Different plasma characteristics were obtained by means of near infrared and UV-visible emission spectroscopy (Figure 1). The near infrared emission spectroscopy and its advantages have been introduced and recently discussed in other studies by our laboratory[4,5].

The near infrared spectra were recorded with a FTLA2000 FTIR (770-3300 nm) spectrometer purchased from ABB-Bomem (Québec, QC, Canada) at a resolution of 2 cm^{-1} corresponding to 0.2 nm at 1000 nm. For near infrared light collection, the IR light exited the reactor through a ZnSe feedthrough window, expanded through a concave ZnSe lens, and was redirected by a concave gold mirror into the FTIR's entrance port. The IR optics were all purchased from International Scientific Products Corp. (Irvington, NY, USA). The detector used during each experiment was a thermoelectrically cooled indium arsenide (InAs) semiconductor diode sensitive in the 710-3300 nm range. The UV–VIS (300–800 nm) emission spectra were recorded at a resolution of 0.75 nm by means of an HR4000 apparatus from Ocean Optics (Dunedin, FL, USA). UV–VIS light emitted by the plasma was collected by a fused silica collimator and transferred via an optical fiber perpendicular to the cylindrical reactor axis into the entrance slit of the spectrometer which was equipped with a 300 grooves/mm^{-1} grating and a CCD detector. In order to improve the signal-to-noise ratio while preventing a saturation of the detector, the integration time was set at 300 ms. Three hundred scans were routinely co-added.

To determine the various plasma parameters, plasma emission spectra were recorded in both the UV-visible and IR regions for each surface treatment for the various plasma process conditions.

3.2 Correlation of the plasma optical emission spectroscopy with surface modification

The correlation between the predictive matrix X (the plasma characteristics) and the response matrix Y (the surface chemistry as determined by XPS and surface derivatization) was determined by applying a PLSR analysis. The PLSR model in this study was built using custom scripts written in the MATLAB R2010a (MathWorks, Inc.) environment with the PLS-Toolbox (Eigenvector Research, Inc.).

These results enable us to highlight the physics and chemistry governing the mechanism behind polymer surface treatment. The process conditions were adjusted prior to each experiment, while the plasma parameters were measured using UV-visible and IR emission spectra. Plasma pressures of 100, 250, 500, 1000, and 2000 mTorr were investigated with $H_2/(N_2+H_2)$ ratios of 0, 0.05, 0.1, 0.2, and 0.4, for a total of 25 experimental conditions. The plasma characteristics were measured for each condition using the approaches described in Section 2. As three replicates were made for each process condition, the X predictor matrix was (75 × 6), while the response matrix consisted of atomic surface concentration data as determined by XPS (%C, %F, %N, $\%NH_2$), and therefore to a Y matrix of (75 × 4).

Of interest here is that according to the experimental results, no clear trend was evident for grafted oxygen on the surface, depending on the plasma process condition. In fact, grafted oxygen on the surface depends not only on the plasma modification process but also on the post-oxidation when the sample is exposed to air at the end of the plasma treatment. Here, because the time of post-oxidation was not constant for the entire surface modification process, the error introduced to these results was relatively high. For this reason, in a multivariate data analysis, the oxygen concentration was removed from the results of the XPS to improve the mathematical modeling results.

4 RESULTS AND DISCUSSION

The surface modifications were performed for different plasma pressures and $H_2/(N_2+H_2)$ ratios. For each experiment with a particular plasma process condition, the UV-visible and IR spectra were acquired simultaneously to determine the various plasma parameters.

4.1 Plasma optical emission spectroscopy

4.1.1 Atomic species density in plasma

To summarize, the relative atomic concentrations of nitrogen and hydrogen as well as the plasma temperature were determined using the near infrared part of the spectrum, while the vibrational temperature calculations of the ground state species in the plasma were obtained from the UV-visible emission spectra.

Figure 2 shows the near infrared spectrum of a 92%-5% N_2-H_2 plasma containing 3% of an actinometer gas (Ar). Various nitrogen, hydrogen, and argon atomic transitions as well as different molecular transitions of nitrogen are clearly observed. As stated, actinometry was used to determine the relative concentration of the atomic ground state of nitrogen and hydrogen in the discharge in various plasma experimental conditions. As previously described[4], the atomic transition lines of nitrogen (λ = 1359 nm), hydrogen (λ = 1875 nm) and argon (λ = 1350 nm) were used.

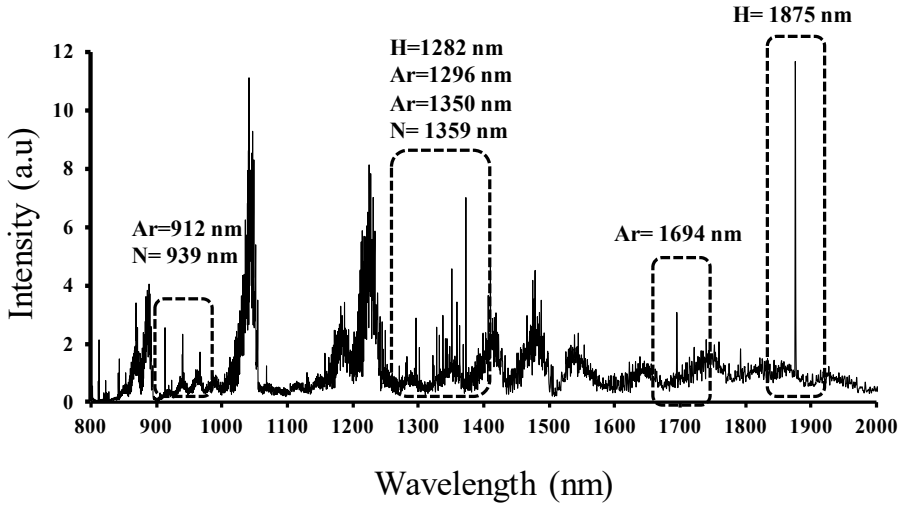


Figure 2. Plasma emission spectra in the 800–2000 nm range. The relative ratios of N_2, H_2 and Ar were 92%, 5% and 3%, respectively. Various atomic transitions are identified by rectangles (300 W, 500 mTorr). Reproduced from ref[4] with permission.

4.1.2 Measurement of the rotational temperature

The near infrared emission spectra were recorded for the investigated plasma conditions and were subsequently used to monitor the rotational temperature which is considered to be close to the plasma temperature. Specifically, this was done by comparing the calculated and experimental spectra in the first positive system of nitrogen with the sequence of $\Delta v = +2$ (1025-1050 nm). Figure 3 shows an example of a measured rovibrational N_2 spectrum along with the corresponding calculated spectrum. As can be seen, an excellent match was observed between the calculated and experimental spectra.

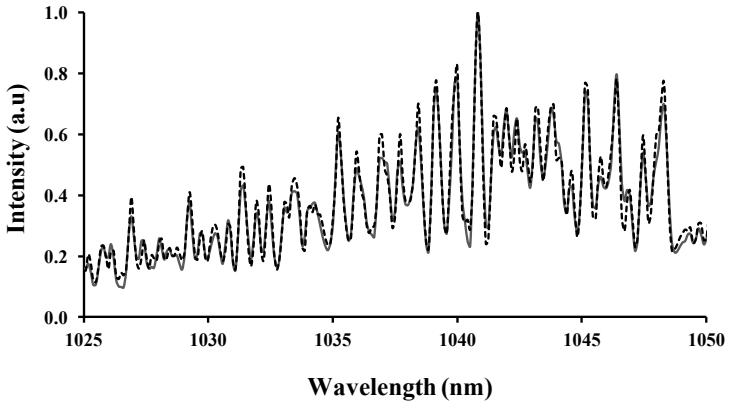


Figure 3. Experimental spectrum (solid line) and corresponding numerically generated spectrum (dotted line) of the 0-0 band for the best fit gas temperature. The evaluated rotational temperature (Tr) was 1009 K (300 W, 3000 mTorr).

4.1.3 Measurement of the vibrational temperature

The various plasma vibrational temperatures were measured by means of the light emission in the UV-visible spectral region which made it possible to determine the characteristic vibrational temperatures $\theta_1(X)$ of N_2 (X,v) from the vibrational distribution of the 2nd positive system of N_2 (C,v'). Figure 4 shows this spectrum for the $\Delta v = +2$ transition. The bands of interest are located at 380.5 (0–2), 375.5 (1–3), 371 (2–4) and 367.2 (3–5) (λ in nm).

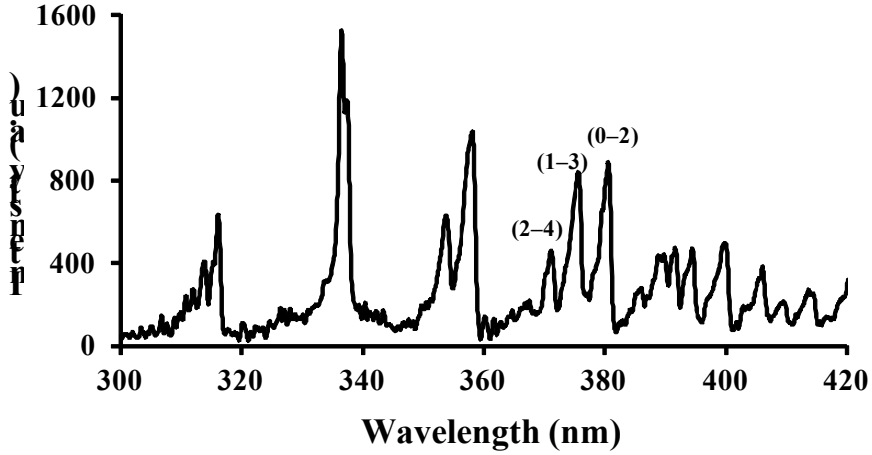


Figure 4. Plasma emission spectrum in the 300–420 nm range along with the $\Delta v = -2$ sequence of N_2 for the bands located at 380.5 (0–2), 375.5 (1–3), and 371 (2–4) (λ in nm) (300 W, 500 mTorr).

4.2 Effect of plasma parameters on the modified surface

All of the surface chemistry results are presented in terms of %F, %C, %N and $\%NH_2$ surface concentration. As N_2 and N_2-H_2 plasmas were used to modify the surface, it was clear that the percentage of nitrogen would be a valid indicator of the extent of the plasma treatment. Moreover, %N probed the extent of nitrogen atom insertion on the PTFE surface, while %F monitored the level of defluorination and was indicative of the amount of fluorine atoms substituted by other atoms and/or by multiple bond formation within or between the polymeric chains. Because the desired species on the surface was NH_2, chemical derivatization was applied to measure the selectivity of the grafting.

Figure 5-a shows the surface modifications observed through XPS on the PTFE samples as depicted by the decrease of the F/C ratio. As can be seen here, a pure N_2 discharge led to only a slight defluorination of the surface, yet greater defluorination was observed at lower pressure. On one hand, introducing 5% of H_2 in the discharge resulted in a significant surface modification of the PTFE. On the other hand, the overall defluorination curve profile was similar for all of the investigated pressures for H_2 concentrations ranging from 0% to 40%, while the rate of defluorination was more significant at a low hydrogen percentage.

Figures 5-b and 5-c, respectively, show the nitrogen and amino group surface concentration profiles as a function of the H_2 concentration for various pressures in the plasma reactor. As can be seen, pure nitrogen enabled the grafting of only a small quantity of nitrogen-containing groups onto the surface, particularly at lower pressures. However, by increasing the pressure from 1000 to 2000 mTorr, the surface remained untreated. Of no surprise is that no surface amino groups were detected on the plasma-treated PTFE surface in the pure N_2 environment due to the absence of any hydrogen-containing species either in the plasma or on the polymer surface.

Incorporating as least 5% of hydrogen in the discharge led to an increase in the amount of both nitrogen-containing species and amino groups, with optimum values reached when the hydrogen concentration within the plasma varied between 5 and 20%, depending on the gas pressure within the plasma chamber.

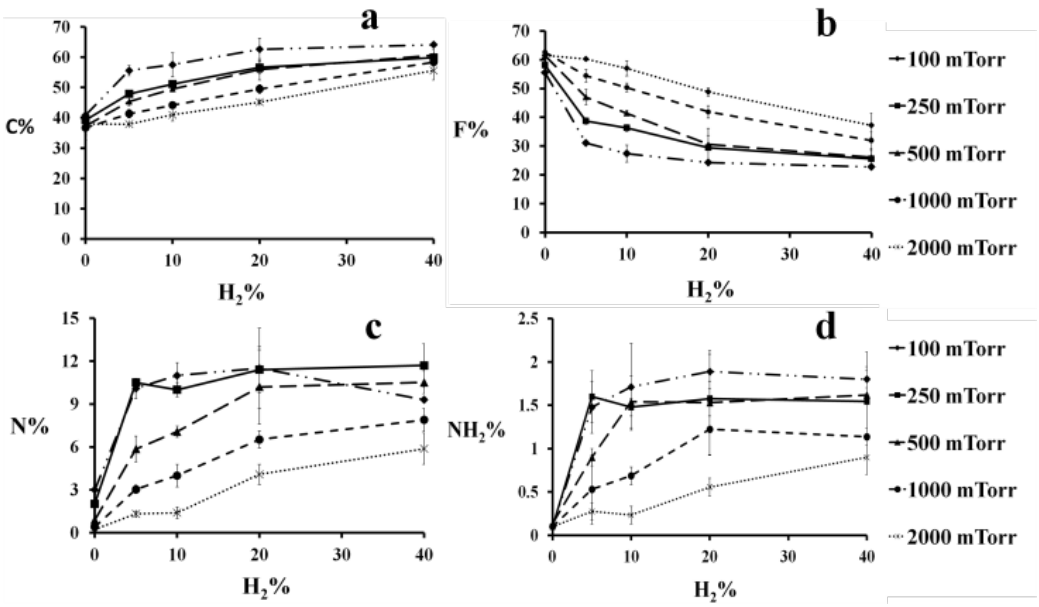


Figure 5. XPS measurement of (a) C%, (b) F%, (c) N% and (d) NH_2% of the PTFE polymer as a function of H_2 and pressure in the discharge (treatment time= 3 min).

4.3 Multivariate analysis (relationships between surface characteristics and process conditions/plasma parameters)

The experimental design presented in Section 3-2 generated a data set of X (75 × 7) containing the plasma characteristics and process conditions for each experiment as well as a corresponding response matrix Y (75 × 4) containing the chemical compositions of the films. As surface treatment was repeated three times for each process condition, one of the replicates was randomly chosen and set aside to form a test set for model predictive ability validation, while the remaining matrix of data was used as the training set to build the PLSR model. Thus, the PLSR was conducted to correlate X_t (50 × 7) to Y_t (50 × 4), while the model predictive ability was assessed on X_v (25 × 7)

and Y_v (25 × 4). These data sets were autoscaled to normalize the units and the range of the variables prior to application of the PLSR.

In order to avoid over-fitting, the number of PLSR components was selected by calculating the root mean squared error (RMSE) of the training (RMSEC) and test (RMSEP) sets for each number of latent variable space:

$$\text{RMSE}=\sqrt{\frac{1}{N}\sum_{i=1}^{N}(y_i-\hat{y}_i)^2} \tag{9}$$

where y_i is the measured value and $\hat{y}_i$ is the predicted value for the i^{th} sample. As depicted in Figure 6, three components were determined for PLSR:

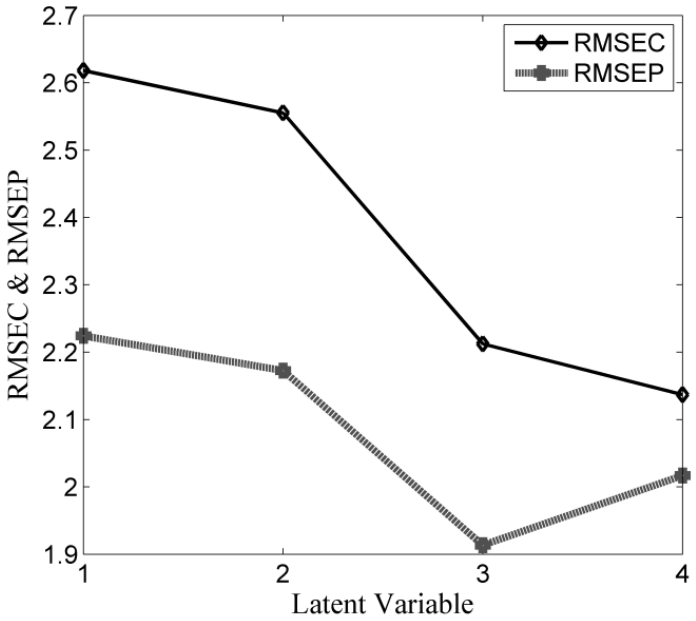


Figure 6. RMSEC and RMSEP versus model complexity (number of principal components).

Our analysis shows that 87.8% of the X_t variance and 75.5% of the Y_t variance were captured by the PLSR model. Table 1 summarizes the prediction results for the multivariate PLSR model on the training and test sets. In this table, the explained variance in the training (R2C) and test (R2P) sets are shown as well as the root mean square errors (RMSEC and RMSEP) and pure error.

R^2C and R^2P, shown here, depict the cumulative variance of each Y-variable as explained by the PLSR mod-el, with 3 components on the test set and the validation set, respectively. In addition, the pure error (equation 10, which is the sum of all standard deviation) was calculated for each of the 75 experiments to compare them with the RMSE of the calibration and prediction (Table 1).

$$SD_{total}=\sqrt{\frac{1}{N}\sum_K\sum_i\left(y_{i,k}-\overline{y_k}\right)^2} \tag{10}$$

The R^2C and R^2P coefficients presented in Table 1 show a good agreement between the actual surface characteristics values and their predicted ones. On the other hand, the findings for %C and %F were more accurate in regard to their RMSEs. The experimental results for N and NH_2 presented greater uncertainty because their absolute surface concentration was much less important than that

of C and F. In addition, regarding to Table 1, pure error and RMSE of the calibration and prediction are in the same range despite the lower values of pure error.

Table 1. Predictive ability of PLSR on the training and test sets.

	%C	%F	%N	$\%NH_2$
RMSEC	3.79	5.53	2.21	0.43
RMSEP	3.96	4.83	1.91	0.37
Pure error	1.57	1.89	0.98	0.21
R^2C	0.83	0.82	0.73	0.64
R^2P	0.82	0.86	0.79	0.70

Of interest here is that our data confirms that it is indeed possible to predict the treated surface chemistry from the plasma characteristics. That being said, the PLSR model could no doubt be improved by adding more information in the input matrix. For example, the energy of the electrons within the plasma certainly influenced the surface modification process. Thus, introducing electron temperature data into the model would most likely have improved it.

The PLSR loading biplot for the first two principal components (Figure 7) made it possible to interpret the relationships between the plasma parameters, processing conditions, and PTFE surface chemical compositions.

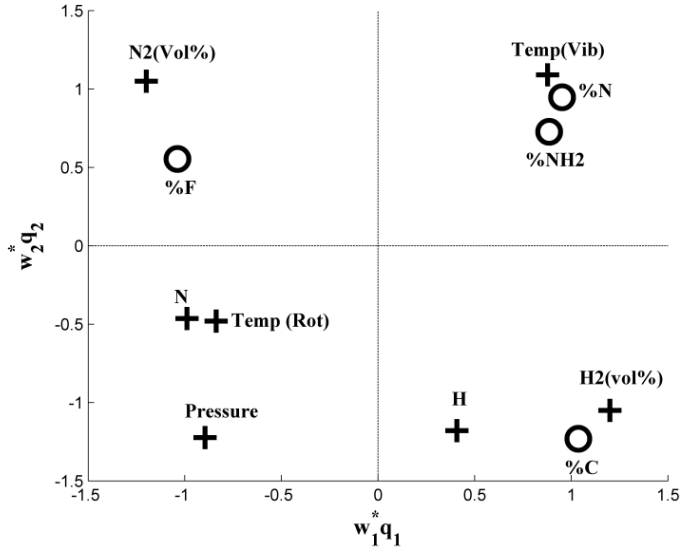


Figure 7. Loading biplot of the first 2 components of the PLSR model depicting the correlation between the plasma parameters, processing conditions, and PTFE chemical compositions.

The PLSR biplot reveals a correlation of variables within each block and between the X and Y block, simultaneously. Variables located in the same quadrant in the biplot were positively correlated, while variables falling in opposite quadrants were negatively correlated. In addition, the distance to the origin conveys information on the impact of variables. The further away a variable lies from the plot origin, the stronger its impact on the model[18]. In other words, the variables located near the region had little impact on the model.

As can be seen in Figure 7, one may deduce that the vibrational temperature was negatively correlated with pressure and rotational temperature. In the experimental results, we observed the same trend, because when the pressure increased, the rotational temperature also increased, while

the vibrational temperature de-creased. According to this biplot, %N and $\%NH_2$ were positively correlated with the vibrational temperature of N_2 while being negatively correlated with the pressure. This is an indication that energetic nitrogen species were indeed involved in the surface defluorination process.

Also in Figure 7, the variations related to the surface chemistry were captured by the first PLSR principal component, which explains the greatest amount of variance in the data (i.e. horizontal axis in Figure 7), as %F was of course negatively correlated to %N, $\%NH_2$, and %C, and this shows the evolution of the chemical reaction. The second PLSR component (vertical axis in Figure 7) rather involved %N and %C which were negatively correlated in this latent variable space.

Additional information on the influence of each of the 7 X-variables in the 3-component PLSR model was obtained through the calculation of the VIPs which are presented in Figure 8.

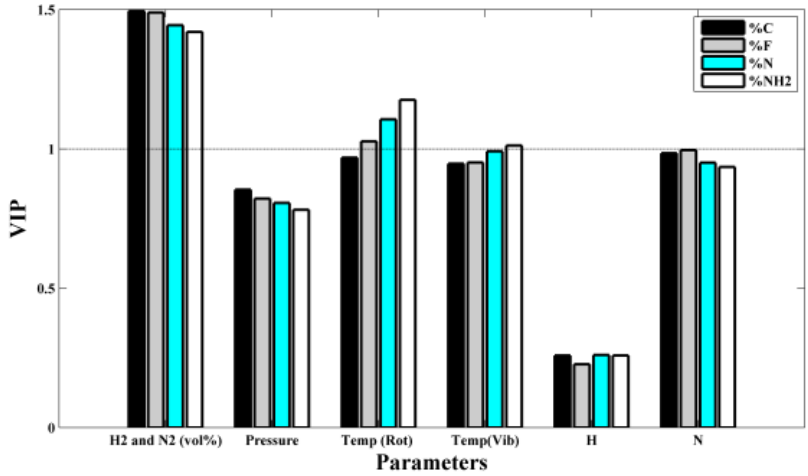


Figure 8. VIP plot showing the relative importance of each X-variable in the PLSR model.

This figure shows that the PLSR model strongly relied on relative N_2 and H_2 gas concentration in the discharge (first and second VIPs), followed by the plasma rotational and vibrational temperature (third and fourth VIP). However, plasma pressure and N atomic concentration in the discharge were less significant on the surface properties. The VIP results indicate that despite the importance of H_2 in the modeling of the system, the H atomic concentration was the least significant for variable projection.

The relationships established between the plasma process parameters/characteristics and the treated PTFE surface chemistry sheds light on the nature of the mechanisms involved in the modification process. The qualitative data presented in Figure 5 indicates that defluorination can indeed occur in a pure N_2 plasma environment, provided the pressure is lower than 1000 mTorr. It therefore appears that the density of $N_2(A)$ species was high enough to transfer the energy (6.2 eV) and break the C-F bonds (5 eV). In addition, the possibility that other energetic nitrogen species may be involved in the defluorination process cannot be ruled out. The dissociation of H_2 added to the discharge into H atoms clearly adds up to the presence of the $N_2(A)$ metastable species to further defluorinate the polymer surface. The radicals created on the polymer are then available to react with gaseous plasma species to lead to amino groups, among others[20].

VIP values nevertheless show that the effect of H atomic concentration within the plasma was much less important than was the H_2 partial pressure for surface functionalization. Regarding this result, one of the possibilities of NH_2 surface grafting may be via NH formation in the discharge. It has been shown that the main mechanism producing NH in this process condition may take place through the following reactions, which indicate the importance of H_2 in the discharge to produce NH or N, which may contribute to surface functionalization[21]:

$$N(^2D) + H_2 \rightarrow H + NH$$
$$N + H_2(v) \rightarrow H + NH$$
$$N + NH \rightarrow H + N_2$$
$$H + NH \rightarrow N + H_2$$

On the other hand, the VIP results show that N atomic concentration and vibrational temperature were more important than was H atomic concentration. Molecules $N_2(X, v)$ were associated with N atoms to treat the surface as the reaction $e + N_2(X, v) = e + N + N$ was favored when $N_2(X, v)$ was high. In this case, a better surface treatment is associated with high values of $N_2(X, v)$ and N. These findings are in agreement with previous research in a microwave discharge showing that the relative contribution of the $N_2(X)$ for dissociation increased rapidly by adding H_2 in the discharge[21].

The present data demonstrate that hydrogen was not directly involved in the defluorination of the surface but rather produced atomic nitrogen and/or $N_2(A)$ or other energetic nitrogen species which were shown to be at the origin of fluorine atom removal from the polymer surface. At this point, the nature of the interaction between N and/or NH and the surface remains to be investigated.

Although the mechanisms presented here may be the dominant ones for surface modifications, they must be further validated by more extensive research addressing the various plasma processes by chemical kinetics modeling and plasma characterization techniques such as Langmuir probing.

It is important to note that this model was developed to highlight the effect of process conditions and plasma characteristics on the chemistry of plasma-treated surfaces. Clearly, this model confirms that process conditions are not the only sources of variations to affect treated surface chemistry. Indeed, plasma characteristics play a definite role and must be considered to optimize the process and predict the surface chemical composition.

5 CONCLUSIONS

This study demonstrates the enormous potential of both UV-visible and IR emission spectroscopy to monitor plasma processes and shed new light on plasma surface modification mechanisms. In addition to plasma process conditions, the plasma characteristics, measured through the so-called spectroscopy methods, may be powerful tools to predict treated surface chemistry and highlight the mechanisms responsible for surface modification. The approach basically consisted in generating a mathematical model through the partial least squares method to correlate an input matrix containing both experimental plasma conditions and plasma characteristics with an output matrix housing XPS surface chemistry data. The correlation coefficient obtained using this mathematical model showed a very good fit between the predicted and actual surface chemistry data and therefore supports the predictive ability of the model. This mathematical procedure also made is possible to determine the VIP values, which somewhat weight the importance of each plasma parameter/characteristic on the resulting surface chemistry, thereby enabling us to identify those mechanisms underlying polymer surface treatment. These results thus confirm that plasma characteristics must be considered to optimize plasma processes and predict surface chemical composition.

To the best of our knowledge, this study is the first to use emission spectroscopy from the light emitted by plasmas to predict the resulting treated polymer chemistry surface.

ACKNOWLEDGEMENTS

The authors acknowledge the financial support from the Natural Sciences and Engineering Research Council of Canada (NSERC) and the Centre Québécois sur les Matériaux Fonctionnels (CQMF). The authors would also like to thank André Ricard for his sup-port and helpful discussions.

REFERENCES

(1) Pringle, S. D.; Joss, V. S.; Jones, C. Ammonia Plasma Treatment of PTFE Under Known Plasma Conditions. Surf. Interface Anal. 1996, 24, 821-829.
(2) Wang, M.J.; Chang, Y.I.; Poncin-Epaillard, F. Effects of the Addition of Hydrogen in the Nitrogen Cold Plasma: The Surface Modification of Polystyrene. Langmuir. 2003, 19, 8325-8330.
(3) Favia, P.; Stendardo, M.; d'Agostino, R. Selective Grafting of Amine Groups on Polyethylene by Means of NH3−H2 RF Glow Discharges. Plasmas Polym. 1996, 1, 91-112.
(4) Mavadat, M.; Turgeon, S.; Ricard, A.; Laroche, G. Infrared Optical Actinometry to Determine N- and H-Atom Density in a N2 –H2 Microwave Discharge. J. Phys. D: Appl. Phys. 2012, 45, 315201.
(5) Mavadat, M.; Ricard, A.; Sarra-Bournet, C.; Laroche, G. Determination of Ro-vibrational Excitations of N2(B, v') and N2(C ,v') States in N2 Microwave Discharges Using Visible and IR Spectroscopy. J. Phys. D: Appl. Phys. 2011, 44, 155207.
(6) Sarra-Bournet, C.; Ayotte, G.; Turgeon, S.; Massines, F.; Laroche, G. Effects of Chemical Composition and the Addition of H2 in a N2 Atmospheric Pressure Dielectric Barrier Discharge on Polymer Surface Functionalization. Langmuir. 2009, 25, 9432-9440.
(7) Fantz, U. Basics of Plasma Spectroscopy. Plasma Sources Sci. Technol. 2006, 15, S137-S147.
(8) Biloiu, C.; Sun, X.; Harvey, Z.; Scime, E. An Alternative Method for Gas Temperature Determination in Nitrogen Plasmas: Fits of the Bands of the First Positive System (B 3Πg→A 3Σu+). J. Appl. Phys. 2007, 101, 073303-073311.
(9) Gardet, G.; Moulard, G.; Courbon, M.; Rogemond, M.; Druetta. M. Evaluation of the Rotational Temperature in N2 Discharges Using Low-Resolution Spectroscopy. Meas. Sci. Technol. 2000, 11, 333-341.
(10) Tonnis, E. J.; Graves, D. B. Neutral Gas Temperatures Measured Within a High-density, Inductively Coupled Plasma Abatement Device. J. Vac. Sci. Technol., A. 2002, 20, 1787-1795.
(11) Marvadat, M.; Turgeon, S.; Ricard, A.; Laroche, G. Characterization of Microwave Plasma for Polymer Surface Modification Using FTIR Emission Spectroscopy, Adv. Mat. Res. 2012, 409, 797-801.
(12) Gordiets, B.; Hamedov, S.; Shelepin, L. Vibrational Kinetics of Harmonic Oscillators Under Essentially Nonequilibrium Conditions. Sov. Phys. J. Exp. Theor. Phys. 1975, 40, 640.
(13) Gat, E.; Gherardi, N.; Lemoing, S.; Massines, F.; Ricard, A. Quenching Rates of N2(C,v') Vibrational States in N2 and He Glow Silent Discharges. Chem. Phys. Lett. 1999, 306, 263-268.
(14) Gilmore, F.R.; Laher, R. R.; Espy, P. J. Franck-Condon Factors, r-Centroids, Electronic Transition Moments, and Einstein Coefficients for Many Nitrogen and Oxygen Band Systems. J. Phys. Chem. Ref. Data. 1992, 21. 1005-1107.
(15) Piper, L. G. Energy Transfer Studies on $N_2(X\,^1\Sigma+g,v)$ and $N_2(B\,^3\Pi g)$. J. Chem. Phys. 1992, 97, 270-275.
(16) Wold, S.; Sjostrom, M.; Eriksson, L. PLS-regression: a Basic Tool of Chemometrics. Chemom. Intell. Lab. Syst. 2001, 58, 109-130.
(17) Höskuldsson, A. PLS Regression Methods. J. Chemometrics. 1988, 2, 211-228.
(18) Eriksson, L.; Johansson, E.; Kettaneh-Wold, N.; Wold, S. Multi- and Megavariate Data Analysis, Principles and Applications, Umetrics Academy, Umea, 2001.
(19) Gaudet, S.; Janes, K. A.; Albeck, J. G.; Pace, E. A.; Lauffenburger, D. A.; Sorger, P. K. A Compendium of Signals and Responses Triggered by Prodeath and Prosurvival Cytokines. Mol. Cell. Proteomics. 2005, 4, 1569-1590.
(20) Klages, C.P.; Grishin, A. Plasma Amination of Low-Density Polyethylene by DBD Afterglows at Atmospheric Pressure. Plasma Proc. Polym. 2008, 5, 368-376.
(21) Tatarova, E.; Dias, F. M.; Gordiets, B.; Ferreira, C. M. Molecular Dissociation in N2-H2 Microwave Discharges. Plasma Sources Sci. Technol. 2005, 14, 19-31.